Neurobiology of Pain 13 (2023) 100120

Contents lists available at ScienceDirect

Neurobiology of Pain

journal homepage: www.sciencedirect.com/journal/neurobiology-of-pain

Modulating the activity of human nociceptors with a SCN10A promoter-specific viral vector tool

Stephanie Mouchbahani-Constance [a,b], Camille Lagard [c], Justine Schweizer [b,d], Isabelle Labonté [e], Miltiadis Georgiopoulos [f], Colombe Otis [g,h], Manon St-Louis [i], Eric Troncy [g,h,j], Philippe Sarret [c,j], Alfredo Ribeiro-Da-Silva [b,i,j], Jean A. Ouellet [b,f], Philippe Séguéla [b,d,j], Marie-Eve Paquet [e,j,k], Reza Sharif-Naeini [a,b,j,*]

[a] Department of Physiology and Cell Information Systems Group, McGill University, Montreal, Canada
[b] Alan Edwards Center for Research on Pain, McGill University, Montreal, Canada
[c] Institut de Pharmacologie de Sherbrooke, Département de Pharmacologie-Physiologie, Faculté de Médecine et des Sciences de la Santé, Université de Sherbrooke, Sherbrooke, Quebec, Canada
[d] Department of Neurology & Neurosurgery, Montreal Neurological Institute/Hospital, Faculty of Medicine and Health Sciences, McGill University, Montreal, Quebec, Canada
[e] CERVO Brain Research Centre, CIUSSS-CN, Quebec, Quebec, Canada
[f] Spine Surgery Program, Department of Surgery, McGill University, Montreal, Canada
[g] Research Group in Animal Pharmacology of Quebec (GREPAQ), Université de Montréal, Saint-Hyacinthe, Quebec, Canada
[h] Department of Veterinary Biomedicine, Faculty of Veterinary Medicine, Université de Montréal, Saint-Hyacinthe, Quebec, Canada
[i] Department of Pharmacology & Therapeutics, McGill University, Montreal, Quebec, Canada
[j] Quebec Consortium on Mapping of Pain Circuits, Quebec, Canada
[k] Department of Biochemistry, Microbiology and Bio-Informatics, Université Laval, Québec, Quebec, Canada

ARTICLE INFO

Keywords:
Pain
Gene therapy
AAV
DREADD
Sodium channel
Chemogenetics
DRG

ABSTRACT

Despite the high prevalence of chronic pain as a disease in our society, there is a lack of effective treatment options for patients living with this condition. Gene therapies using recombinant AAVs are a direct method to selectively express genes of interest in target cells with the potential of, in the case of nociceptors, reducing neuronal firing in pain conditions. We designed a recombinant AAV vector expressing cargos whose expression was driven by a portion of the SCN10A ($Na_V1.8$) promoter, which is predominantly active in nociceptors. We validated its specificity for nociceptors in mouse and human dorsal root ganglia and showed that it can drive the expression of functional proteins. Our viral vector and promoter package drove the expression of both excitatory or inhibitory DREADDs in primary human DRG cultures and in whole cell electrophysiology experiments, increased or decreased neuronal firing, respectively. Taken together, we present a novel viral tool that drives expression of cargo specifically in human nociceptors. This will allow for future specific studies of human nociceptor properties as well as pave the way for potential future gene therapies for chronic pain.

Introduction

Chronic pain is a prevalent disease estimated to affect 1 in 5 people worldwide (Middleton et al., 2021). Its prevalence is matched with the lack of efficacious and tolerable treatment options for patients afflicted with the disease. In many chronic pain conditions, the pathology is due in large part to excessive activity of nociceptors themselves. In these "nociceptor-driven" chronic pain conditions, a considerable research effort is underway to define their underlying mechanisms in the hopes of identifying novel therapeutic strategy to help those patients. However, an alternative approach to treating nociceptor-driven chronic pain conditions can be to bypass the original receptor or molecular mechanism affected and simply block the nociceptor's ability to send electrical signals to the central nervous system.

One of the most efficient ways to do this is to specifically silence the entire neuron using hyperpolarizing actuators, such as the inhibitory DREADDs (designer receptors exclusively activated by designer drugs) hM4Di (human M4 muscarinic Gi-coupled DREADD) independently of

* Corresponding author at: Department of Physiology and Cell Information Systems Group, McGill University, Montreal, Canada.
E-mail address: reza.sharif@mcgill.ca (R. Sharif-Naeini).

https://doi.org/10.1016/j.ynpai.2023.100120
Received 11 December 2022; Received in revised form 25 January 2023; Accepted 25 January 2023
Available online 30 January 2023

the pathological mechanism at play. The advantage of such an approach is that it can target multiple nociceptor-driven chronic pain subtypes. However, such an ambitious endeavour requires the ability to specifically target nociceptors. This is no small feat since the human dorsal root ganglia (hDRG) comprise at least 12 different subtypes of sensory neurons (Tavares-Ferreira et al., 2022), and 11 neuronal subtypes have been identified in the mouse DRG (mDRG) (Usoskin et al., 2014). Each subtype differs in a variety of factors including the diameter of the cell body, the degree of myelination of its peripheral and central terminals and, most importantly, in its pattern of expression of ion channels and receptors (Tavares-Ferreira et al., 2022; Usoskin et al., 2014). The unique complement of ion channels expressed by the different subsets of hDRG neurons can therefore be leveraged to design adeno-associated viruses (AAVs) driving the expression of inhibitory actuators under the control of nociceptor-specific promoters.

These AAVs are found in multiple vertebrate species (including humans) and do not seem to cause any human diseases, making them a good candidate for viral gene delivery in the central and peripheral nervous system (Wang et al., 2019). Recombinant AAVs (rAAVs) are devoid of nearly all AAV protein-coding sequences and have an exogenous gene expression cassette inserted in their place. The only remaining genes guide genome replication and packaging. This transforms the rAAV into a membrane-crossing, gene-encoded protein-based nanoparticle that can efficiently perform the transfer of DNA cargo into the nuclei of target cells (Knipe et al., 2013; Naso et al., 2017; Wu et al., 2006; Asokan et al., 2012; Dunbar et al., 2018; Burger et al., 2004). This removal of viral coding sequences contributes to their low immunogenicity when injected *in vivo* (Wang et al., 2019). These benefits make rAAVs the leading platform for delivering gene therapies *in vivo*, with the first rAAV-based gene therapy product (Luxturna) obtaining FDA approval in 2017 (Wang et al., 2019). Many other rAAV-based treatment options are in the pipeline for a variety of conditions including, but not limited to, treatments for hemophilia B (George et al., 2017; Herzog et al., 1997; Mount et al., 2002; Nathwani et al., 2011; Nathwani et al., 2014), lipoprotein lipase deficiency (Gaudet et al., 2013), Parkinson's disease (Christine et al., 2009; Hwu et al., 2012; Muramatsu et al., 2010) and retinal blindness (Bainbridge et al., 2008; Bainbridge et al., 2015; Bennett et al., 2016; Hauswirth et al., 2008; Jacobson et al., 2015; Maguire et al., 2009; Russell et al., 2017; Wright, 2015). Treatment specificity is achieved by engineering the viral DNA to drive the expression of a gene of interest (GOI) under the control of a cell-specific promoter to maximize its therapeutic potential. In the context of nociceptor-driven chronic pain conditions, pain sensing neurons located in the DRG are particularly good candidates for gene therapy due to the high density of blood vessels and the lack of a protective surrounding capsular membrane (Knipe et al., 2013; Naso et al., 2017; Wu et al., 2006; Asokan et al., 2012; Dunbar et al., 2018; Burger et al., 2004; Berta et al., 2017; Jurczak et al., 2021). These factors make the DRG accessible via systemic administration routes.

By modifying the choice of promoter controlling the expression of the viral cargo, one can specifically target expression of a GOI to a genetically distinct cell type (Burger et al., 2004; Dong et al., 2010; O'Carroll et al., 2020). The promoter region of the voltage-gated sodium channel $Na_V1.8$ (*SCN10A* gene) was recently identified and shown to be predominantly active in neural crest-derived sensory neurons, which corresponds to nociceptors (Lu et al., 2015). Recent spatial transcriptomics sequencing data on human DRGs has shown that SCN10A is seemingly expressed in *all* human nociceptor subtypes and lowly expressed in C-LTMRs (Goodwin and McMahon, 2021; Han et al., 2016), without being expressed in other, non-pain related sensory DRG neuron subtypes such as proprioceptors or other low-threshold mechanoreceptors (LTMRs: Aβ SA LTMRs, Aβ RA LTMRs and Aδ LTMRs). Another isoform, SCN11a, was also shown to be expressed somewhat specifically in human nociceptors, but its expression levels in non-nociceptor neurons was slightly higher than that of SCN10A, further reinforcing that SCN10A may be a more specific promoter for the treatment of chronic pain (Tavares-Ferreira et al., 2022).

Here, we leveraged this discovery to generate viral vectors that can be used to selectively target actuators to human nociceptors to control their excitability. We first confirmed the vector's specificity to $Na_V1.8$-positive neurons in mice, then performed experiments on human DRG neurons to 1) confirm the virus efficacy at infecting human neurons, 2) the specific expression of the virus cargo in nociceptors, and 3) verify whether the virus can effectively express actuators that allow us to modulate the activity of human nociceptors.

Methods

Animals

All animal procedures were approved by the Institutional Animal Care and Use Committee for McGill University. For intraperitoneal injections, $Na_V1.8$-Cre × ChR2-EYFP male pups, produced from a cross between Ai32(RCL-ChR2(H134R)/EYFP) (C57BL/6J, Jackson Labs, strain # 012569) and $Na_V1.8$-Cre mice (obtained from Dr. Mohammed Nassar (Stirling et al., 2005), were used at P5, and the same genotype and sex was used for intrathecal injections at 4 weeks of age. For intrasciatic injections, male flex-tdTom mice (C57/Bl6j background, Jackson Laboratory strain #007914) were used at 8 weeks of age. Animals were housed in a temperature-controlled room under a 12 h light/dark cycle. Water and food were available *ad libitum*.

Injections

For intraperitoneal injections, 5 μL of AAV2/8-SCN10A-mCherry (titer = 5.7 E12 gc/mL) were injected using a Hamilton syringe into the intraperitoneal space of $Na_V1.8$-Cre × ChR2-EYFP pups previously anesthetized on ice. For intrathecal injections, 2 μL of AAV2/8-SCN10A-mCherry were injected between L5 and L6 of anesthetized (isoflurane) $Na_V1.8$-Cre × ChR2-EYFP mice. For intrasciatic injections, 2 μL of AAV2/8-SCN10A-CRE virus (titer = 8.0 E12 gc/mL) were injected into the sciatic nerve of anesthetized (isofluorane) flex-tdTom mice. In all cases, animals were kept under observation until fully recovered from anesthesia. 4-week-old and older mice were all placed on warming mat during injections (intrasciatic and intrathecal) and left on mat during recovery from anesthesia to ensure conservation of body heat and optimal recovery. Mice were perfused with 4 % paraformaldehyde (PFA) and DRGs were dissected 3–4 weeks after injections for immunostaining and fluorescence imaging.

Tissue preparation

For all fluorescence imaging and immunohistochemistry (IHC) experiments, mice were deeply anesthetized with isoflurane before being transcardially perfused with 10 mL of phosphate-buffered saline (PBS), followed by 25 mL of 4 % PFA in 0.1 M phosphate buffer. Their L3 and L4 DRGs were dissected and post-fixed in 4 % PFA for 1 h, followed by cryoprotection in a 30 % sucrose solution in PBS for 72 h. The DRGs were then embedded in optimal cutting temperature compound (OCT) and cut into 14 μm-thick transverse sections with a cryostat (Thermo Scientific, Waltham, MA, Microm HM525 NX Cryostat) directly onto microscope slides.

Immunohistochemistry

Immunostaining was performed directly on microscope slides containing cryosectioned DRG slices. Using a hydrophobic barrier, slides were washed twice for 10 min, first with PBS and second with 0.33 % PBS-Triton. Sections were then blocked for 1 h in 10 % NGST (composed of 10 % normal goat serum diluted in PBS-Triton) at room temperature with constant gentle shaking. Sections were then washed for 10 min in PBS-Triton and then incubated for 48 h with primary antibodies at 4 °C

on a shaker in 1 % NGST. The following primary antibodies and concentrations were used: Alexa-488 Isolectin-B4 conjugate (1:500 diluted in 1 % NGST, Invitrogen #I21411) and rabbit anti-βIII-tubulin (1:500 diluted in 1 % NGST, Novus Biologicals #NB600-936). Sections were then washed for 15 min 3 times with 1 % NGST and then incubated with the secondary antibody, Alexa-647 goat anti-rabbit (1:1000 diluted in 1 % NGST, Invitrogen #A32733), for 1 h at room temperature with gentle shaking. Slides were washed again for 15 min, 3 times, and then incubated with DAPI for 10 min at room temperature (NucBlue, Invitrogen #R37605). Finally, slides were washed for 5 min, 3 times, in PBS and then rinsed once with distilled water before being left to dry and coverslipped using Fluoromount-G (SouthernBioTech, Birmingham, AL) as mounting media.

Generation of adeno associated viral vector constructs

A plasmid containing the DNA sequence for the SCN10A promoter was obtained from H.L. Puhl III and the 3.5 Kb fragment was subcloned in the pAAV backbone (Lu et al., 2015). The cDNA encoding either mCherry, CRE or eGFP were then cloned downstream of the promoter to generate 3 different plasmids. Plasmid pAAV-CAG-DIO-hM3Dq-mCherry was modified from B. Roth's material (University of North Carolina, Chapel Hill, USA). All constructs were verified by sequencing and correct clones were amplified in Stbl2 *E. coli* and the DNA was purified in endotoxin-free conditions.

Generation of recombinant AAV

Briefly, AAVs were generated in HEK293T17 cells by a triple transfection of helper plasmid pXX680, a plasmid containing the AAV2/8 Rep/Cap and the plasmids described above. 72 h post transfection, the culture medium was harvested, debris centrifuged out and viral particles concentrated through a tangential flow filter. Free DNA was digested with Benzonase and viral particles purified by a discontinuous gradient of iodixanol (15–25-40–60 %) and ultracentrifugation (70,000 RMP 1 h30 at 16 °C). The viral preparation was then concentrated through a Centricon filter and adjusted to 5 % sorbitol and 0.001 % Pluronic acid for storage and experimentation. Titration was performed by digital droplet-PCR using primers specific for AAV2 ITR.

Fluorescence microscopy

Fluorescence imaging of tissue from $Na_V1.8$-Cre × ChR2-EYFP mouse DRGs (injected with virus) was performed using a Zeiss Axio Imager.M2 with a Zeiss colibri 7 light source and a high-resolution Zeiss Axiocam 512 monochrome camera. Images were taken using a Zeiss 2.6 (blue edition) software. Imaging of immunohistochemistry was performed using an LSM 710 Confocal microscope equipped with Ar and HeNe lasers using a 10x and 20x objectives. All cell counting analyses were performed using a macro in ImageJ. Statistical analyses were performed by generating a mean number of cells per mouse, and then comparing different groups based on mean values for each mouse.

Human dorsal root ganglion collection and culture

Collection of human dorsal root ganglia (hDRGs) was approved by the McGill University Ethical Review Board (IRB# A04-M53-08B) in collaboration with Transplant Quebec Organ Donation. Dorsal root ganglia were collected in oxygenated NMDG-aCSF following a thoracolumbar spine harvest (T10/11 to L5S1) no more than 4 h after aortic cross-clamp. Electrophysiological recordings were performed on hDRG neurons obtained from 5 organ donors, comprised of 3 males (ages 20, 51, and 61) and 2 females (ages 18 and 62) with neurological death as the cause of death.

Primary hDRG cultures were generated and maintained using an adapted version of the protocol published by Valtcheva et al. (Valtcheva et al., 2016). Briefly, after collection in oxygenated NMDG-aCSF, hDRGs were dissected by removing the dura as well as the central and peripheral nerve bundles and then minced in small (roughly 2 mm × 2 mm) pieces using a scalpel. The DRG fragments were then incubated at 37 °C for 1 h 45 min in a pre-warmed solution composed of 0.2 % collagenase type IV (Sigma-Aldrich Cat#: c1889) and 0.2 % dispase type II (Sigma-Aldrich Cat#: 04693) diluted in NMDG-aCSF. After the incubation, DRG fragments were rinsed 3 times with 3 mL of warmed NMDG-aCSF and placed in 2 mL of warmed human DRG media. Human DRG media was composed of Neurobasal A media (Gibco cat#: 21103049) with 1 % Penicillin/Streptomycin (Wisent Bioproducts Cat#: 450–201 EL), 2 % B-27 supplement (Gibco Cat#: 12587–010), 5 % FBS (Wisent Bioproducts Cat#: 80150) and 1 % GlutaMAX (Gibco Cat#: 35050–061). DRGs were then triturated with a plastic transfer pipette pre-absorbed with FBS and then passed through a 100 mm cell strainer in a 50 mL Falcon tube. Cells were then centrifuged at 180 g for 4 min, pellet re-suspended in 1 mL DRG media and centrifuged again at 180 g for 3 min. Cells were plated on 35 mm glass bottom m-dishes (Ibidi #81156) at a density of roughly 1 DRG for every 10 dishes with a central drop of 250 mL per dish. Cells were incubated at 37 °C, 5 % CO_2 for 1 h to allow neurons to adhere before filling each dish with 1 mL of media. Neurons were maintained at 37 °C, 5 % CO_2 with half of the culture media replaced every 2 days and using AraC (1 mM) as needed to remove satellite glial cells from the culture. Any electrophysiology or calcium imaging experiments were performed a minimum of 3 days after initial plating to ensure that satellite glial cells peeled off neurons to allow for membrane access and were kept in culture for up to 14 days.

Calcium imaging

Changes in intracellular calcium concentrations in single cells were recorded as change in GCaMP7s fluorescence by exciting the sample with 480-nm light every second. Images were collected using a 40X objective (Olympus, Tokyo, Japan) with a CoolSNAP MYO camera (Photometrics, Tucson, AZ). The MetaFluor software (Molecular Devices Version 7.7) was used for data acquisition. Cells were imaged in normal extracellular solution (in mM): 140 NaCl, 3 KCl, 1 $MgCl_2$, 1 $CaCl_2$, 10 HEPES and 10 Glucose; in distilled water, buffered to a pH of 7.3 with NaOH. Capsaicin (Sigma-Aldrich Cat#: M2026), αβMe-ATP (Cayman Chemicals Cat# 10008956) and KCl were superfused using a fast solution exchanger (Harvard Apparatus #SF-77B). Capsaicin was prepared at a concentration of 10 μM, αβMe-ATP at a concentration of 3 μM and KCl was prepared at a solution of 80 mM with 10 mM HEPES in distilled water. Cells were considered to have a positive response to the application of αβMe-ATP, capsaicin or KCl when their intracellular calcium concentration rose by at least 20 % over baseline values within 5 s of compound application. To record changes in intracellular calcium, cells were transduced with AAV2/8-SCN10A-CRE (titer = 8.0 E12 gc/mL) and AAV2/9-CAG-flex-jGCaMP7s (titer = 1.5 E13 gc/mL).

Electrophysiology

Whole-cell patch clamp electrophysiology was performed on hDRGs 72 h after preparation of the primary cell culture and infection with different viruses. Viruses used included AAV2/8-SCN10A-eGFP (titer = 1.5 E13 gc/mL), AAV2/8-SCN10A-CRE (titer = 8.0 E12 gc/mL), AAV2/8-CAG-DIO-hM3D-mCherry (titer = 1.3 E13 gc/mL) and AAV2/9-CAG-DIO-hM4D-mCherry (titer = 1.5 E13 gc/mL). All viruses were used in human DRG cultures with an MOI of 2. The extracellular solution contained (in mM): 140 NaCl, 3 KCl, 1 $MgCl_2$, 1 $CaCl_2$, 10 HEPES, 10 Glucose (pH 7.3 with NaOH and 315 mOsm with Mannitol). Recording electrodes were made using fire-polished glass pipettes (AM Systems, Glass Borosilicate, 1.5 mm OD, 0.86 ID) with resistances of 5 – 7 MOhms. Recording electrodes were filled with a solution containing (in mM): 130 K-gluconate, 5 KCl, 5 NaCl, 3 Mg-ATP, 0.3 EGTA, 10 HEPES (pH 7.3 with KOH and 305 mOsm with Mannitol). Observations were

made on an Olympus IX71 inverted microscope with a MultiClamp 700B (Axon CNS, Molecular Devices, Sunnyvale, CA, USA) amplifier and Digidata 1440A (Molecular Devices) digitizer. Membrane current and voltage were acquired and amplified via the MultiClamp and Digidata and were sampled at 10 kHz. Signals were recorded with Clampex10 and MultiClamp 700B software, then analyzed using Clampfit10. For all recordings, pipette and membrane capacitance were compensated for with the auto function of Clampex10.

After obtaining a gigaOhm seal and transitioning to the whole-cell current clamp configuration, neurons were stimulated with 20 sweeps of increasing current steps lasting 200 ms starting with −100 pA, increasing in 100 pA intervals to 1800 pA. Neurons were then recorded in a gap-free protocol with 0 pA of current injection and were recorded for 1 min to measure their resting membrane potential (RMP). In the same recording, they were then exposed to the hM3Dq agonist Compound-21 (C21, applied in bath solution at a concentration of 1 mM), for 60 more seconds. The mean RMP of the cells was recorded both before application of C21 and in the presence of C21. At the end of this gap-free recording, the current step protocol was repeated. The number of action potentials per step of current injection was quantified for each the pre- and post-C21 groups and plotted in an input–output curve as a function of the injected current. For experiments using C21 (Hello Bio,

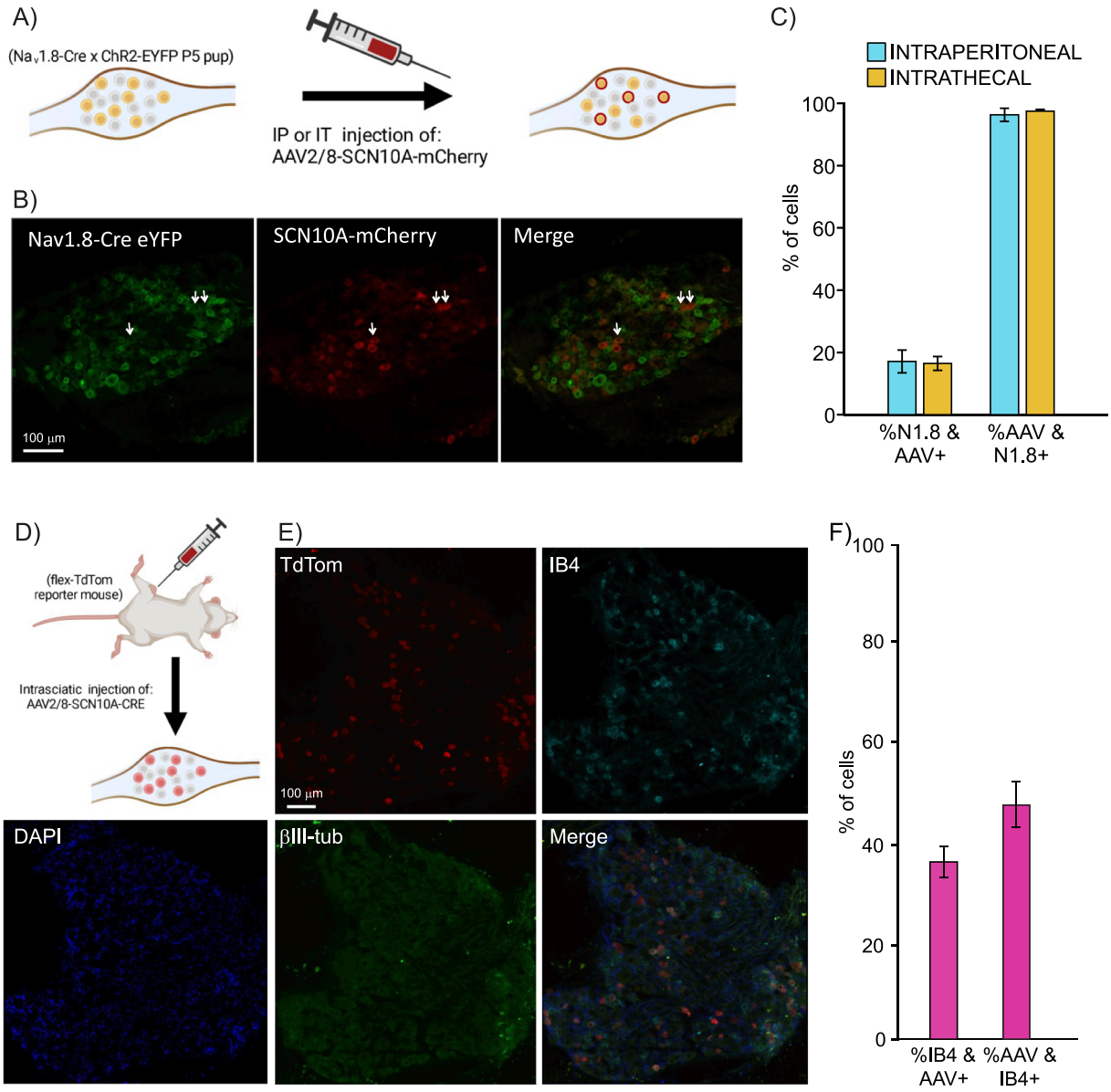

Fig. 1. The AAV2/8-SCN10A-mCherry virus specifically infects DRG cells that express the $Na_V1.8$ sodium channel, half of which seem to be non-peptidergic nociceptors. A) Schematic demonstrating expected results from injection of SCN10a-driven virus in $Na_V1.8$-CrexChR2-EYFP P5 pups. B) Representative image of a DRG extracted from a $Na_V1.8$-Cre × ChR2-eYFP pup injected with virus as described in panel A. eYFP-driven fluorescence from $Na_V1.8$-Cre mouse (left) and mCherry-driven fluorescence driven by SCN10a virus (middle) with both images merged on the right. C) Quantification of proportion of eYFP ($Na_V1.8$)-positive cells that are also mCherry (AAV)-positive (left 2 bars, 804/5151 and 858/5404 cells total, respectively), and quantification of proportion of mCherry (AAV)-positive cells that are also eYFP ($Na_V1.8$)-positive (right 2 bars, 804/823 and 858/861 cells total, respectively). Both intraperitoneal and intrathecal injection routes were tested, both gave similar results. N = 3 mice for each the intraperitoneal and intrathecal injections. D) Schematic showing expected results from injection of SCN10a-Cre virus in flex-tdTom reporter mice. E) Immunohistochemistry of a DRG from a flex-TdTom reporter mouse injected intrasciatically with AAV2/8-SCN10A-Cre. TdTom fluorescence is driven by the virus' expression, Isolectin-B4 was used to identify non-peptidergic nociceptors and βIII-tubulin was used to provide context along with DAPI. E) Quantification of proportion of IB4 neurons that are AAV (tdTom)-positive (left) (381/994 cells total from n = 3 mice) and proportion of AAV (tdTom)-positive neurons that are IB4-positive (381/806 total cells). Data are represented as Mean +/- SEM.

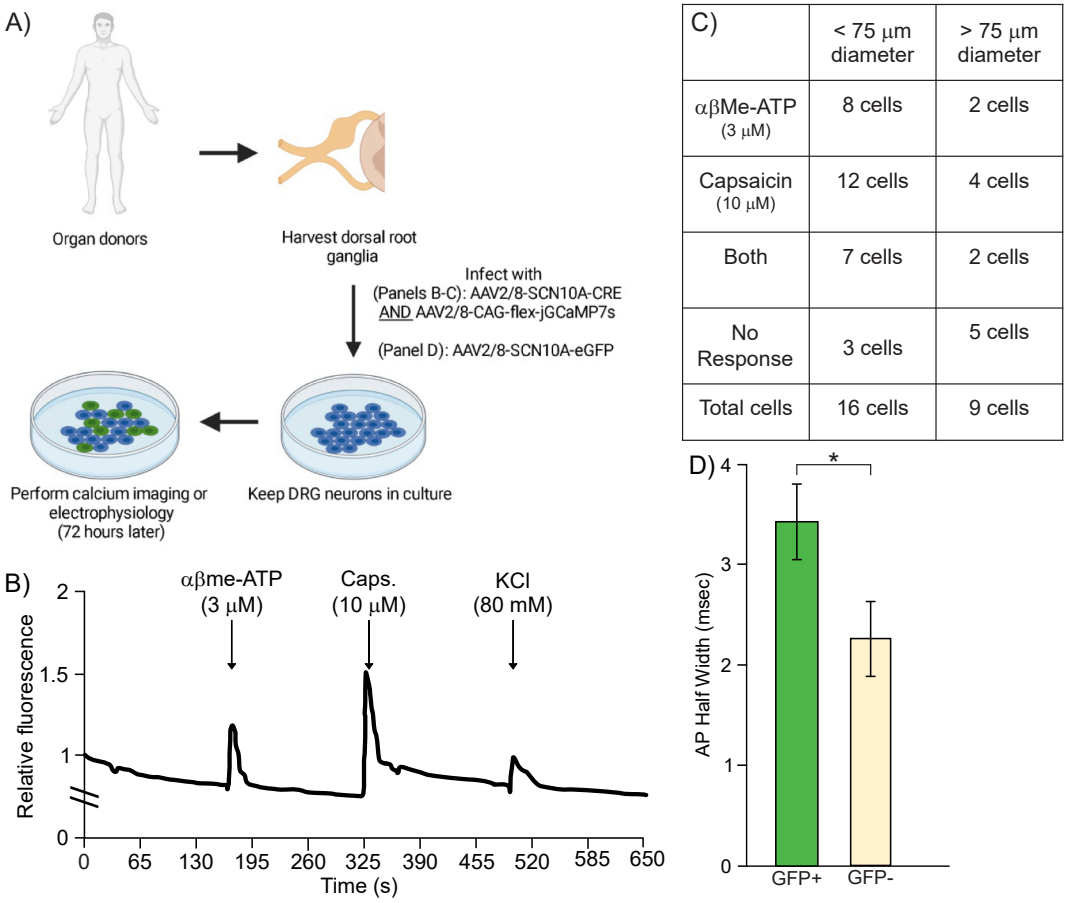

Fig. 2. The virus AAV2/8-SCN10A-Cre successfully transduces human sensory neurons, which appear to be nociceptors, and drives the expression of functional GCaMP7s for calcium imaging. A) Schematic of experimental plan. B) Sample trace of calcium imaging using GCaMP7s, whose expression was driven by AAV2/8-SCN10a-Cre along with an AAV2/8-CAG-flex-GCaMP7s in human DRG neurons. Cells expressing GCaMP7s can successfully demonstrate a rise in intracellular calcium following applications of common algogens such as αβMe-ATP and Capsaicin. C) Quantification of number of infected human DRG neurons, classified based on the diameter of their soma, responding to αβMe-ATP, capsaicin, both or no response. n = 25 cells in total. D) Quantification of action potential half-width in human DRG neurons infected with an AAV2/8-SCN10a-GFP virus (n = 4 GFP-positive neurons) or that did not get infected with the virus (n = 5 GFP-negative neurons). * $p < 0.05$ (unpaired *t*-test).

#HB6124), C21-dihydrochloride was initially prepared in 100 mM aliquots in H_2O. On the day of experiments, 100 mM aliquots were diluted to 1 μM in extracellular solution and then superfused over the cells through a fast solution exchanger (Harvard Apparatus #SF-77B).

Data analysis and diagrams

All drawings (Fig. 1A and D, Fig. 2A, Fig. 3A) were made with BioRender. Statistical analyses were performed using Python with the following packages: scipy, pandas, seaborn and numpy. Significant differences were determined using either paired or unpaired t-tests, 1-way or 2-way ANOVAs depending on the experiment with appropriate post hoc tests, described in the results section. The significance threshold was set to $p < 0.05$.

Results

The SCN10A promoter targets expression specifically in $Na_V1.8$-positive neurons

To validate that SCN10A promoter-driven expression is restricted to $Na_V1.8$-expressing neurons, we packaged the promoter along with the mCherry cDNA into an AAV2/8 vector and injected it in $Na_V1.8$-Cre × ChR2-EYFP mice. In the latter, all $Na_V1.8$-expressing neurons also express the fluorescent protein EYFP. We performed intraperitoneal (injected in pups at P5) or intrathecal (injected in 4-week-old mice) injections of AAV2/8-SCN10A-mCherry virus (Fig. 1A). Four weeks later, we quantified the degree of co-localization of the EYFP tag, originating from embryonic $Na_V1.8$ expression, and the mCherry tag, originating from the virus, driven by activity of the $Na_V1.8$ promoter (Fig. 1B). Overall, in our intraperitoneal injection group, we found that out of 10,585 total cells from 3 mice, 5151 (48.67 %) were EYFP-positive, indicating embryonic expression of $Na_V1.8$, and 823 (15.98 %) were mCherry-positive, indicating that they were successfully infected with our virus. In our intrathecal injection group, we found that out of 10,303 total cells from 3 mice, 5404 (52.45 %) were EYFP-positive and 861 (8.36 %) were mCherry-positive. We observed that 97.69 ± 0.74 % (804/823 cells total from n = 3 mice) and 99.65 ± 0.19 % (858/861 cells total from n = 3 mice) of mCherry-positive neurons from mice that received an intraperitoneal or intrathecal injection, respectively, were also EYFP-positive (Fig. 1C, right bars). This demonstrates that while the virus may infect many neurons in the vicinity of the injection site, its cargo, driven by the SCN10A promoter, will only be expressed in neurons expressing $Na_V1.8$.

We also observed that 15.6 ± 1.27 % (804/5151 cells total from n = 3 mice) and 15.88 ± 0.90 % (858/5404 cells total from n = 3 mice) of EYFP-positive neurons were also mCherry-positive in DRGs from mice that received an intraperitoneal or intrathecal injection, respectively (Fig. 1C, left bars). This is likely because not all neurons that expressed $Na_V1.8$ embryonically continue to express the gene in adulthood, thus

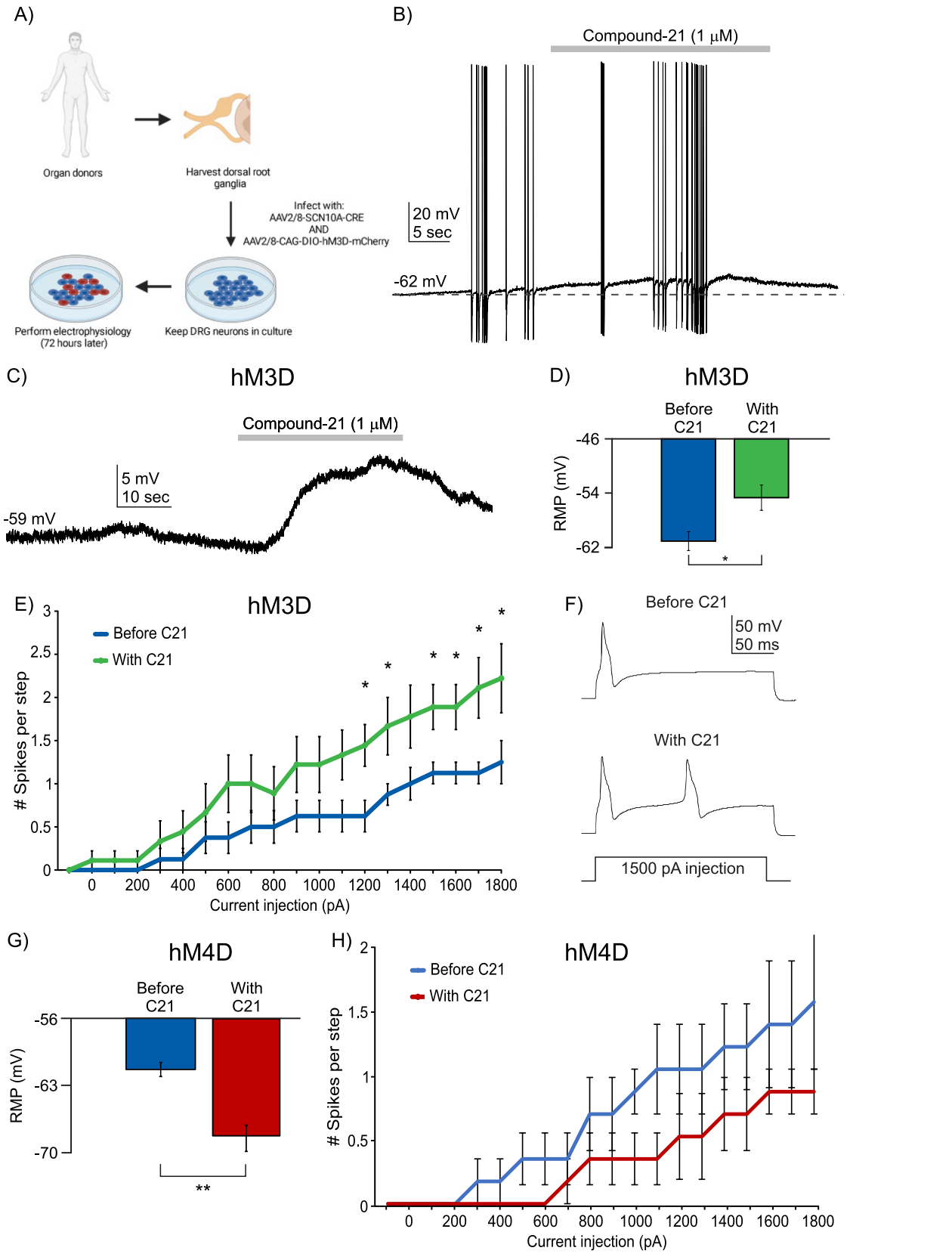

(caption on next page)

Fig. 3. Human DRG neuron excitability can be modulated by SCN10a-promoter-driven actuators in AAV2/8 viral constructs. A) Schematic of experimental plan. B) Sample trace of current clamp recording of a human DRG neuron infected by both AAV2/8-SCN10a-Cre and AAV2/8-CAG-DIO-hM3D-mCherry viruses. Application of Compound-21 (C21, agonist of hM3D) can increase firing rates of human DRG neurons infected with both viruses. C) Sample trace of gap-free current clamp recording of a human DRG neuron infected by hM3D dual virus approach and showing depolarization upon application of C21. D) Quantification of mean resting membrane potential (RMP) in mV of human DRG neurons infected with hM3D dual virus approach before C21 (blue bar) and after C21 (green bar). * $p < 0.05$, paired *t*-test. E) Input-output curve of human DRG neurons infected with hM3D dual virus approach before C21 (blue line, n = 8 neurons) and after C21 (green line, n = 8 neurons) following a current step protocol. * $p < 0.05$. Two-way ANOVA followed by the Tukey post hoc test. F) Representative trace of spikes in an m-Cherry-positive neuron before and after application of C21 in response to a 1500 pA step of current injection. G) Quantification of mean resting membrane potential (RMP) in mV of human DRG neurons infected with hM4D dual virus approach before C21 (blue bar) and after C21 (red bar). ** $p < 0.021$, paired *t*-test. H) Input-output curve of human DRG neurons infected with hM4D dual virus approach before C21 (blue line, n = 6 neurons) and after C21 (red line, n = 6 neurons) following a current step protocol. Two-way ANOVA followed by the Tukey post hoc test, no significant differences.

failing to engage the SCN10A promoter contained in the virus. Taken together, these results confirm that a viral vector whose cargo is under the control of the SCN10A promoter can specifically bring this cargo in $Na_V1.8$-expressing neurons and does so with a similar penetrance between the intraperitoneal or intrathecal injection route.

The SCN10A promoter confers cargo expression in a mixed population of neurons, half of which are non-peptidergic nociceptors

To gain more specific insights into the subtypes of neurons in which the SCN10A promoter confers cargo expression, we performed intrasciatic injections of AAV2/8-SCN10A-Cre into 8-week-old flex-TdTomato reporter mice (n = 3 mice) (Fig. 1D). When SCN10A-driven Cre expression occurs in these neurons, the floxed stop cassette upstream of the tdTomato gene is excised and the red fluorescent protein is expressed. Mice were perfused 3 weeks post virus injection and their L3 and L4 DRGs were dissected, sectioned, and stained in IHC experiments to reveal the identity of the tdTomato-positive neurons. Markers used in this experiment included IB4 (labels non-peptidergic nociceptors), beta-III tubulin (labels all neurons), and DAPI (Fig. 1E). Of the total population of IB4-positive neurons (994/4283 total DRG cells from n = 3 mice), 37.97 ± 6.17 % (381/994 total cells from n = 3 mice) were also tdTom-positive (Fig. 1F). On the other hand, 47.64 ± 5.97 % (381/806 total cells from n = 3 mice) of neurons expressing tdTom (804/4283 total cells from n = 3 mice) were co-labeled with IB4, indicating that approximately half of the population of neurons that engaged the SCN10A promoter were non-peptidergic nociceptors, corresponding to just over one third of the global non-peptidergic nociceptor population (Fig. 1F). This is consistent with single-cell RNA sequencing data of the adolescent mouse DRG (mousebrain.org; (Zeisel et al., 2018)which has shown that approximately half of the neurons that express $Na_V1.8$ in the DRG are non-peptidergic nociceptors, with the other half being peptidergic nociceptors (Zeisel et al., 2018).

The SCN10A promoter-containing viral vector can successfully drive the expression of functional proteins in human nociceptors

To confirm the translational potential of rAAV use for modulating the activity of nociceptors, we sought to infect primary cultures of hDRG neurons with our SCN10A promoter-containing virus and evaluate its ability to 1) express functional proteins, 2) restrict expression to human nociceptors and 3) express proteins that enable the modulation of the excitability of human nociceptors. First, we determined the most effective AAV serotype for infecting hDRG neurons by culturing them with a variety of AAV serotypes that expressed eGFP (independent of SCN10A promoter activity) (see supplemental Fig. 1) and confirmed that AAV2/8 was among the most effective serotypes at infecting human neurons, followed closely by AAV2/9.

To characterize the human neurons expressing SCN10A-driven cargo, we functionally classified then using a dual-virus approach aimed at getting these neurons to express the calcium indicator jGCaMP7s. Primary hDRG cultures were infected with both AAV2/8-SCN10A-CRE and AAV2/8-CAG-flex-jGCaMP7s so that only cells infected with both viruses and that have engaged the SCN10A promoter would express jGCaMP7s (Fig. 2A). After incubating hDRG neurons with the two viruses for 72 h, we performed calcium imaging and recorded baseline fluorescence for 1 min before briefly applying, every 3 min, 3 μM αβMethylene-ATP (αβMe-ATP) to verify P2X3 ATP-gated channel expression, then 10 μM capsaicin to verify TRPV1 channel expression, and 80 mM KCl to confirm that the cell being imaged was indeed a neuron (see sample trace in Fig. 2B). Cells that did not display a rise in intracellular calcium following an application of KCl were excluded from our analysis.

A total of 25 neurons were imaged from 4 different donors, 16 had a diameter under 75 μm and 9 had a diameter larger than 75 μm. In the first group (<75 μm), 8 cells responded to αβMe-ATP, 12 to capsaicin and 7 to both algogens (Fig. 2C). Three cells responded to neither algogen but did respond to KCl, indicating that they were functional neurons. Importantly, all cells that expressed jGCaMP7s also responded to KCl (not shown), indicating that the virus cargo was expressed only in neurons and not in satellite or other glial cells. In the second neuronal group (>75 μm), 2 cells responded to αβMe-ATP, 4 to capsaicin and both αβMe-ATP-responding neurons displayed a rise in intracellular calcium in response to both capsaicin and αβMe-ATP (Fig. 2C). Five cells responded to neither αβMe -ATP nor capsaicin but did respond to KCl (Fig. 2C). While in mice, P2X3 and TRPV1 are not widely expressed together in nociceptors, recent spatial transcriptomic data has shown that almost all human nociceptors seem to express *TRPV1*, significantly overlapping with the population of neurons expressing SCN10A and showing some overlap with the population of cells expressing *P2RX3* (Tavares-Ferreira et al., 2022). Overall, these human spatial transcriptomics data support the distribution of channels observed in our calcium imaging assays on $Na_V1.8$-expressing human neurons.

To further confirm that the SCN10A promoter drives cargo expression in human nociceptors over other subtypes of DRG neurons, we examined another feature that is specific to nociceptors: the width of the action potential (AP). In rodents, non-peptidergic nociceptors tend to have a "shoulder" or widening of the AP during the falling phase (Davidson et al., 2014). Human DRG neurons have been observed to have a shoulder quite broadly across groups, however the size of this shoulder varies based on different subtypes of neurons (a clear correlation has yet to be shown between the size of the AP shoulder with the different DRG neuron subtypes in humans) (Davidson et al., 2014). Nevertheless, we quantified the size of the AP half-width in neurons infected with AAV2/8-SCN10A-eGFP and compared it to the AP half-width of cells in the same dish that were exposed to the virus but did not express the SCN10A promoter. We observed a significant difference between these groups: eGFP-positive neurons (n = 6 neurons) had a mean AP half-width of 3.42 (±0.15) msec and eGFP-negative neurons (n = 5 neurons) had a mean AP half-width of 2.25 (±0.19) msec, with a p-value of 0.012 (unpaired *t*-test) (Fig. 2D). Taken together, these data suggest that the Scn10a promoter drives cargo expression in neurons with a larger AP half-width than cells that are not transduced by the virus.

Viral vectors carrying the SCN10A promoter allow for specific modulation of human nociceptor excitability

Finally, we sought to verify if we could use our viral package to control the excitability of human nociceptors. Because of the relatively large size of the SCN10A promoter and the limited packing capacity of the rAAV, we could not insert both the promoter and the excitatory hM3Dq DREADD in the same virus. We therefore used a dual virus approach again, where we incubated hDRG neurons with a AAV2/8-SCN10A-Cre and AAV2/8-CAG-DIO-hM3Dq-mCherry, kept the neurons in culture for 72 h to allow cargo expression, and then performed whole-cell patch clamp electrophysiology on mCherry-expressing neurons (Fig. 3B – F). To activate hM3Dq, we used the biologically inert DREADD agonist Compound-21 (C21) at a concentration of 1 mM for 30 s at a time. In the presence of C21, mCherry-positive neurons depolarized (Fig. 3B – C) and increased their firing rates during short periods of evoked APs (firing activity was evoked by the injection of a depolarizing current of 250 pA) (Fig. 3B). In the absence of APs, C21 depolarized mCherry-positive neurons (Fig. 3C) and significantly depolarized their resting membrane potentials [from −61.12 (±1.40) mV to −54.69 (±1.87) mV (n = 8; p = 0.0166, paired two-tailed *t*-test)] (Fig. 3D). When nociceptors were stimulated with incremental current injection, those expressing mCherry showed significantly more APs once exposed to C21 (n = 8; $p < 0.05$, Two-way ANOVA with Tukey's post hoc test) (Fig. 3E and F).

We next examined whether our dual virus approach could be used to reduce the excitability of nociceptors, by driving the expression of the inhibitory DREADD, hM4Di, selectively in these neurons. We incubated cultured hDRG neurons with both AAV2/8-SCN10A-CRE and AAV2/9-CAG-DIO-hM4Di-mCherry. We found that cells expressing mCherry had significantly hyperpolarized resting membrane potentials after exposure to C21 (-61.2 ± 0.72 mV before C21 exposure vs −67.85 ± 1.08 mV after C21 exposure, n = 6; p = 0.002 paired two-tailed *t*-test, Fig. 3G). Furthermore, while we did not observe a significant difference in the number of spikes per step during our current step protocol (Fig. 3H; n = 6), there was a clear downward trend in the number of evoked action potentials per step in mCherry-positive, hM4Di-expressing human DRG neurons.

Taken together, these data show that we have developed a viral tool and promoter carrier that successfully delivers functional cargo to human nociceptors and that this tool can be used to modulate the activity of these human nociceptors.

Discussion

Devising approaches to specifically target subsets of sensory neurons to modulate their activity remains an important goal in the treatment of chronic pain. Major advances in RNA sequencing and other adjacent technologies have led to great strides in our understanding of the heterogeneity of human sensory neurons (Tavares-Ferreira et al., 2022; Usoskin et al., 2014; Lu et al., 2015; Valtcheva et al., 2016; Davidson et al., 2014; Hartung et al., 2021). These studies played a critical role in enabling a series of subsequent work that have pushed for targeted approaches in the treatment of chronic pain.

Here, we used the recently identified SCN10A promoter (Lu et al., 2015) to selectively target the expression of actuators to the nociceptor population. Overall, the DRGs appear to be good physiological targets for virally-delivered genetic cargos, considering the fact that they are surrounded by a high density of blood vessels and lack a lot of the capsular surroundings that render other tissues less accessible via systemic administration routes (Berta et al., 2017; Jurczak et al., 2021). In our context, the SCN10A promoter was packaged in an AAV vector with high affinity for human nociceptors and tested for expression specificity in mouse and human DRG neurons. In the latter, we demonstrated that if the promoter drove the expression of a neuronal silencer, such as the inhibitory DREADD hM4Di, exposing human nociceptors to the ligand C21 led to membrane hyperpolarization and a decrease in neuronal firing rate. The advantage of this technique is that it overlooks the sensory pathway that is sensitized in nociceptors, whether it is heat, cold, or mechanical hypersensitivity, and reduces the ability of nociceptors to transmit the electrical input to the spinal cord. The approach can therefore be used to treat a broad variety of chronic pain conditions, if they depend on nociceptor input. Furthermore, this tool can be used to perform highly tuned studies of subsets of nociceptors and can be adapted for use in pain relief for larger animals, primates or even humans.

Some studies have taken a different approach to gene delivery, using *ex vivo* delivery routes using cellular engineering (Middleton et al., 2021). These approaches can be very effective, as they typically use a patient's own cells, reducing any potential immunogenic side effects. However, these labor-intensive, costly, and time-consuming approaches are typically specific to individuals and the same cells cannot be used for different patients. Viral therapies such as the one we have demonstrated in this study allow for broad treatment of a variety of pain conditions in a variety of different patients with different medical profiles.

Finally, some evidence of non neuronal expression of SCN10A were reported, including in the heart. Indeed, although wide association studies have found associations between genetic variants in or near SCN10A and cardiac arrhythmias (Nielsen et al., 2018; Bezzina et al., 2013), the channel's expression or function in the heart are barely detectable or absent (Casini et al., 2019; Stroud et al., 2016). Furthermore, disrupting the *SCN10A* gene or $Na_V1.8$ function with pharmacological tools in cardiac cells led to inconsistent results on their electrical properties (Casini et al., 2019; Stroud et al., 2016; Verkerk et al., 2012). One possible explanation for the genetic association studies may be that some genetic variants may modulate the expression of the neighboring *SCN5A* gene, which encodes the cardiac $Na_V1.5$ channel (van den Boogaard et al., 2014).

This approach will nonetheless require significant optimization. First, the size of the SCN10A promoter takes a significant portion of the packaging space of the virus, making it difficult to insert a silencing actuator in the same virus. In our experiments, we had to resort to using two viruses, one carrying SCN10A-driven Cre recombinase and another one carrying Cre-dependent hM4Di. This difficulty can be bypassed if we identify cell-specific enhancer sequences (Nord and West, 2020), which confer cell specificity and have much shorter lengths. Second, our validation of the AAV function in human nociceptors was restricted to *in vitro* co-culture experiments. We have not examined whether administration of the AAV led to a neuroimmune reaction. Validation of the immunogenic profile of AAVs is an essential step that can be performed in larger animal models (Klinck et al., 2017), before this approach can be brought closer to clinical use. Although the use of both hM4Di and hM3Dq has been validated for basic science research (Zhang et al., 2022), further studies would be required to (1) determine the effect of long term silencing on cell viability, and (2) determine whether the excessive silencing of nociceptors can increase the risk of injuries, somewhat akin to congenital insensitivities to pain conditions (McDermott et al., 2019).

In conclusion, we present here a novel viral tool that allows for the specific targeting of mouse and human nociceptors, and for the modulation of these neurons' activity. These findings pave the way for future studies to leverage this specific expression system to deliver specific proteins in human nociceptors or allow researchers and clinicians to develop gene therapy tools that can modulate the activity of human sensory neurons *in vivo*.

CRediT authorship contribution statement

Stephanie Mouchbahani-Constance: Investigation, Visualization. **Camille Lagard:** Investigation, Visualization. **Justine Schweizer:** Investigation, Visualization. **Isabelle Labonté:** Investigation, Visualization. **Miltiadis Georgiopoulos:** . **Colombe Otis:** Investigation,

Visualization. **Manon St-Louis:** Investigation, Visualization. **Eric Troncy:** Conceptualization, Methodology, Validation, Formal analysis, Investigation, Supervision, Resources, Funding acquisition. **Phillipe Sarret:** Conceptualization, Methodology, Validation, Formal analysis, Investigation, Supervision, Resources, Funding acquisition. **Alfredo Ribeiro-Da-Silva:** Conceptualization, Methodology, Validation, Formal analysis, Investigation, Supervision, Resources, Funding acquisition. **Jean A. Ouellet:** . **Philippe Séguéla:** Conceptualization, Methodology, Validation, Formal analysis, Investigation, Supervision, Resources, Funding acquisition. **Marie-Eve Paquet:** Conceptualization, Methodology, Validation, Formal analysis, Investigation, Supervision, Resources, Funding acquisition. **Reza Sharif-Naeini:** Conceptualization, Methodology, Validation, Formal analysis, Investigation, Supervision, Resources, Funding acquisition.

Declaration of Competing Interest

The authors declare that they have no known competing financial interests or personal relationships that could have appeared to influence the work reported in this paper.

Data availability

Data will be made available on request.

Acknowledgments

This work was supported by a CIHR grant (CIHR PJT-173355) to RSN, a network initiative grant from the Quebec Pain Research Network for the Quebec Consortium on mapping of pain circuits, and a Vanier PhD Scholarship to SMC.

Appendix A. Supplementary data

Supplementary data to this article can be found online at https://doi.org/10.1016/j.ynpai.2023.100120.

References

Asokan, A., Schaffer, D.V., Samulski, R.J., 2012. The AAV vector toolkit: poised at the clinical crossroads. Mol. Ther. 20, 699–708. https://doi.org/10.1038/mt.2011.287.

Bainbridge, J.W.B., Smith, A.J., Barker, S.S., Robbie, S., Henderson, R., Balaggan, K., Viswanathan, A., Holder, G.E., Stockman, A., Tyler, N., et al., 2008. Effect of gene therapy on visual function in Leber's congenital amaurosis. N. Engl. J. Med. 358, 2231–2239. https://doi.org/10.1056/NEJMoa0802268.

Bainbridge, J.W.B., Mehat, M.S., Sundaram, V., Robbie, S.J., Barker, S.E., Ripamonti, C., Georgiadis, A., Mowat, F.M., Beattie, S.G., Gardner, P.J., et al., 2015. Long-term effect of gene therapy on Leber's congenital amaurosis. N. Engl. J. Med. 372, 1887–1897. https://doi.org/10.1056/NEJMoa1414221.

Bennett, J., Wellman, J., Marshall, K.A., McCague, S., Ashtari, M., DiStefano-Pappas, J., Elci, O.U., Chung, D.C., Sun, J., Wright, J.F., et al., 2016. Safety and durability of effect of contralateral-eye administration of AAV2 gene therapy in patients with childhood-onset blindness caused by RPE65 mutations: a follow-on phase 1 trial. Lancet 388, 661–672. https://doi.org/10.1016/S0140-6736(16)30371-3.

Berta, T., Qadri, Y., Tan, P.-H., Ji, R.-R., 2017. Targeting dorsal root ganglia and primary sensory neurons for the treatment of chronic pain. Expert Opin. Ther. Targets 21, 695–703. https://doi.org/10.1080/14728222.2017.1328057.

Bezzina, C.R., Barc, J., Mizusawa, Y., Remme, C.A., Gourraud, J.-B., Simonet, F., Verkerk, A.O., Schwartz, P.J., Crotti, L., Dagradi, F., et al., 2013. Common variants at SCN5A-SCN10A and HEY2 are associated with Brugada syndrome, a rare disease with high risk of sudden cardiac death. Nat. Genet. 45, 1044–1049. https://doi.org/10.1038/ng.2712.

Burger, C., Gorbatyuk, O.S., Velardo, M.J., Peden, C.S., Williams, P., Zolotukhin, S., Reier, P.J., Mandel, R.J., Muzyczka, N., 2004. Recombinant AAV viral vectors pseudotyped with viral capsids from serotypes 1, 2, and 5 display differential efficiency and cell tropism after delivery to different regions of the central nervous system. Mol. Ther. 10, 302–317. https://doi.org/10.1016/j.ymthe.2004.05.024.

Casini, S., Marchal, G.A., Kawasaki, M., Nariswari, F.A., Portero, V., van den Berg, N.W. E., Guan, K., Driessen, A.H.G., Veldkamp, M.W., Mengarelli, I., et al., 2019. Absence of Functional Nav1.8 Channels in Non-diseased Atrial and Ventricular Cardiomyocytes. Cardiovasc. Drugs Ther. 33, 649–660. https://doi.org/10.1007/s10557-019-06925-6.

Christine, C.W., Starr, P.A., Larson, P.S., Eberling, J.L., Jagust, W.J., Hawkins, R.A., VanBrocklin, H.F., Wright, J.F., Bankiewicz, K.S., Aminoff, M.J., 2009. Safety and tolerability of putaminal AADC gene therapy for Parkinson disease. Neurology 73, 1662–1669. https://doi.org/10.1212/WNL.0b013e3181c29356.

Davidson, S., Copits, B.A., Zhang, J., Page, G., Ghetti, A., Gereau, R.W., 2014. Human sensory neurons: Membrane properties and sensitization by inflammatory mediators. Pain 155, 1861–1870. https://doi.org/10.1016/j.pain.2014.06.017.

Dong, B., Nakai, H., Xiao, W., 2010. Characterization of genome integrity for oversized recombinant AAV vector. Mol. Ther. 18, 87–92. https://doi.org/10.1038/mt.2009.258.

Dunbar, C.E., High, K.A., Joung, J.K., Kohn, D.B., Ozawa, K., Sadelain, M., 2018. Gene therapy comes of age. Science 359. https://doi.org/10.1126/science.aan4672.

Gaudet, D., Méthot, J., Déry, S., Brisson, D., Essiembre, C., Tremblay, G., Tremblay, K., de Wal, J., Twisk, J., van den Bulk, N., et al., 2013. Efficacy and long-term safety of alipogene tiparvovec (AAV1-LPLS447X) gene therapy for lipoprotein lipase deficiency: an open-label trial. Gene Ther. 20, 361–369. https://doi.org/10.1038/gt.2012.43.

George, L.A., Sullivan, S.K., Giermasz, A., Rasko, J.E.J., Samelson-Jones, B.J., Ducore, J., Cuker, A., Sullivan, L.M., Majumdar, S., Teitel, J., et al., 2017. Hemophilia B Gene Therapy with a High-Specific-Activity Factor IX Variant. N. Engl. J. Med. 377, 2215–2227. https://doi.org/10.1056/NEJMoa1708538.

Goodwin, G., McMahon, S.B., 2021. The physiological function of different voltage-gated sodium channels in pain. Nat. Rev. Neurosci. 22, 263–274. https://doi.org/10.1038/s41583-021-00444-w.

Han, C., Huang, J., Waxman, S.G., 2016. Sodium channel Nav1.8: Emerging links to human disease. Neurology 86, 473–483. https://doi.org/10.1212/WNL.0000000000002333.

Hartung, J.E., Moy, J.K., Loeza-Alcocer, E., Nagarajan, V., Jostock, R., Christoph, T., Schroeder, W., and Gold, M.S. (2021). Voltage gated calcium channels in human dorsal root ganglion neurons. Pain *Publish Ahead of Print*. 10.1097/j.pain.0000000000002465.

Hauswirth, W.W., Aleman, T.S., Kaushal, S., Cideciyan, A.V., Schwartz, S.B., Wang, L., Conlon, T.J., Boye, S.L., Flotte, T.R., Byrne, B.J., et al., 2008. Treatment of leber congenital amaurosis due to RPE65 mutations by ocular subretinal injection of adeno-associated virus gene vector: short-term results of a phase I trial. Hum. Gene Ther. 19, 979–990. https://doi.org/10.1089/hum.2008.107.

Herzog, R.W., Hagstrom, J.N., Kung, S.H., Tai, S.J., Wilson, J.M., Fisher, K.J., High, K.A., 1997. Stable gene transfer and expression of human blood coagulation factor IX after intramuscular injection of recombinant adeno-associated virus. Proc. Natl. Acad. Sci. U. S. A. 94, 5804–5809. https://doi.org/10.1073/pnas.94.11.5804.

Hwu, W.-L., Muramatsu, S.-I., Tseng, S.-H., Tzen, K.-Y., Lee, N.-C., Chien, Y.-H., Snyder, R.O., Byrne, B.J., Tai, C.-H., and Wu, R.-M., 2012. Gene therapy for aromatic L-amino acid decarboxylase deficiency. Sci. Transl. Med. *4*, 134ra61. 10.1126/scitranslmed.3003640.

Jacobson, S.G., Cideciyan, A.V., Roman, A.J., Sumaroka, A., Schwartz, S.B., Heon, E., Hauswirth, W.W., 2015. Improvement and decline in vision with gene therapy in childhood blindness. N. Engl. J. Med. 372, 1920–1926. https://doi.org/10.1056/NEJMoa1412965.

Jurczak, A., Delay, L., Barbier, J., Simon, N., Krock, E., Sandor, K., Agalave, N.M., Rudjito, R., Wigerblad, G., Rogóż, K., et al., 2021. Antibody-induced pain-like behavior and bone erosion: links to subclinical inflammation, osteoclast activity and ASIC3-dependent sensitization. Pain. https://doi.org/10.1097/j.pain.0000000000002543.

Klinck, M.P., Mogil, J.S., Moreau, M., Lascelles, B.D.X., Flecknell, P.A., Poitte, T., Troncy, E., 2017. Translational pain assessment: could natural animal models be the missing link? Pain 158, 1633–1646. https://doi.org/10.1097/j.pain.0000000000000978.

Knipe, D.M., Howley, P.M., Griffin, D.E., Lamb, R.A., Martin, M.A., Roizman, B., Straus, S.E.F., 2013. Virology 1 and 2.

Lu, V.B., Ikeda, S.R., Puhl 3rd, H.L., 2015. A 3.7 kb fragment of the mouse Scn10a gene promoter directs neural crest but not placodal lineage EGFP expression in a transgenic animal. J. Neurosci. 35, 8021–8034. https://doi.org/10.1523/JNEUROSCI.0214-15.2015.

Maguire, A.M., High, K.A., Auricchio, A., Wright, J.F., Pierce, E.A., Testa, F., Mingozzi, F., Bennicelli, J.L., Ying, G.-S., Rossi, S., et al., 2009. Age-dependent effects of RPE65 gene therapy for Leber's congenital amaurosis: a phase 1 dose-escalation trial. Lancet 374, 1597–1605. https://doi.org/10.1016/S0140-6736(09)61836-5.

McDermott, L.A., Weir, G.A., Themistocleous, A.C., Segerdahl, A.R., Blesneac, I., Baskozos, G., Clark, A.J., Millar, V., Peck, L.J., Ebner, D., et al., 2019. Defining the Functional Role of NaV1.7 in Human Nociception. Neuron 101, 905–919.e8. https://doi.org/10.1016/j.neuron.2019.01.047.

Middleton, S.J., Barry, A.M., Comini, M., Li, Y., Ray, P.R., Shiers, S., Themistocleous, A. C., Uhelski, M.L., Yang, X., Dougherty, P.M., et al., 2021. Studying human nociceptors: from fundamentals to clinic. Brain. https://doi.org/10.1093/brain/awab048.

Mount, J.D., Herzog, R.W., Tillson, D.M., Goodman, S.A., Robinson, N., McCleland, M.L., Bellinger, D., Nichols, T.C., Arruda, V.R., Lothrop Jr, C.D., et al., 2002. Sustained phenotypic correction of hemophilia B dogs with a factor IX null mutation by liver-directed gene therapy. Blood 99, 2670–2676. https://doi.org/10.1182/blood.v99.8.2670.

Muramatsu, S.-I., Fujimoto, K.-I., Kato, S., Mizukami, H., Asari, S., Ikeguchi, K., Kawakami, T., Urabe, M., Kume, A., Sato, T., et al., 2010. A phase I study of aromatic L-amino acid decarboxylase gene therapy for Parkinson's disease. Mol. Ther. 18, 1731–1735. https://doi.org/10.1038/mt.2010.135.

Naso, M.F., Tomkowicz, B., Perry 3rd, W.L., Strohl, W.R., 2017. Adeno-Associated Virus (AAV) as a Vector for Gene Therapy. BioDrugs 31, 317–334. https://doi.org/10.1007/s40259-017-0234-5.

Nathwani, A.C., Tuddenham, E.G.D., Rangarajan, S., Rosales, C., McIntosh, J., Linch, D. C., Chowdary, P., Riddell, A., Pie, A.J., Harrington, C., et al., 2011. Adenovirus-associated virus vector-mediated gene transfer in hemophilia B. N. Engl. J. Med. 365, 2357–2365. https://doi.org/10.1056/NEJMoa1108046.

Nathwani, A.C., Reiss, U.M., Tuddenham, E.G.D., Rosales, C., Chowdary, P., McIntosh, J., Della Peruta, M., Lheriteau, E., Patel, N., Raj, D., et al., 2014. Long-term safety and efficacy of factor IX gene therapy in hemophilia B. N. Engl. J. Med. 371, 1994–2004. https://doi.org/10.1056/NEJMoa1407309.

Nielsen, J.B., Thorolfsdottir, R.B., Fritsche, L.G., Zhou, W., Skov, M.W., Graham, S.E., Herron, T.J., McCarthy, S., Schmidt, E.M., Sveinbjornsson, G., et al., 2018. Biobank-driven genomic discovery yields new insight into atrial fibrillation biology. Nat. Genet. 50, 1234–1239. https://doi.org/10.1038/s41588-018-0171-3.

Nord, A.S., West, A.E., 2020. Neurobiological functions of transcriptional enhancers. Nat. Neurosci. 23, 5–14. https://doi.org/10.1038/s41593-019-0538-5.

O'Carroll, S.J., Cook, W.H., Young, D., 2020. AAV Targeting of Glial Cell Types in the Central and Peripheral Nervous System and Relevance to Human Gene Therapy. Front. Mol. Neurosci. 13, 618020 https://doi.org/10.3389/fnmol.2020.618020.

Russell, S., Bennett, J., Wellman, J.A., Chung, D.C., Yu, Z.-F., Tillman, A., Wittes, J., Pappas, J., Elci, O., McCague, S., et al., 2017. Efficacy and safety of voretigene neparvovec (AAV2-hRPE65v2) in patients with RPE65-mediated inherited retinal dystrophy: a randomised, controlled, open-label, phase 3 trial. Lancet 390, 849–860. https://doi.org/10.1016/S0140-6736(17)31868-8.

Stirling, L.C., Forlani, G., Baker, M.D., Wood, J.N., Matthews, E.A., Dickenson, A.H., Nassar, M.A., 2005. Nociceptor-specific gene deletion using heterozygous NaV1.8-Cre recombinase mice. Pain 113, 27–36. https://doi.org/10.1016/j.pain.2004.08.015.

Stroud, D.M., Yang, T., Bersell, K., Kryshtal, D.O., Nagao, S., Shaffer, C., Short, L., Hall, L., Atack, T.C., Zhang, W., et al., 2016. Contrasting Nav1.8 Activity in Scn10a-/- Ventricular Myocytes and the Intact Heart. J. Am. Heart Assoc. 5 https://doi.org/10.1161/JAHA.115.002946.

Tavares-Ferreira, D., Shiers, S., Ray, P.R., Wangzhou, A., Jeevakumar, V., Sankaranarayanan, I., Cervantes, A.M., Reese, J.C., Chamessian, A., Copits, B.A., et al., 2022. Spatial transcriptomics of dorsal root ganglia identifies molecular signatures of human nociceptors. Sci. Transl. Med. 14 https://doi.org/10.1126/scitranslmed.abj8186.

Usoskin, D., Furlan, A., Islam, S., Abdo, H., Lönnerberg, P., Lou, D., Hjerling-Leffler, J., Haeggström, J., Kharchenko, O., Kharchenko, P.V., et al., 2014. Unbiased classification of sensory neuron types by large-scale single-cell RNA sequencing. Nat. Neurosci. 18, 145. https://doi.org/10.1038/nn.3881.

Valtcheva, M.V., Copits, B.A., Davidson, S., Sheahan, T.D., Pullen, M.Y., McCall, J.G., Dikranian, K., Gereau 4th, R.W., 2016. Surgical extraction of human dorsal root ganglia from organ donors and preparation of primary sensory neuron cultures. Nat. Protoc. 11, 1877–1888. https://doi.org/10.1038/nprot.2016.111.

van den Boogaard, M., Smemo, S., Burnicka-Turek, O., Arnolds, D.E., van de Werken, H. J.G., Klous, P., McKean, D., Muehlschlegel, J.D., Moosmann, J., Toka, O., et al., 2014. A common genetic variant within SCN10A modulates cardiac SCN5A expression. J. Clin. Invest. 124, 1844–1852. https://doi.org/10.1172/JCI73140.

Verkerk, A.O., Remme, C.A., Schumacher, C.A., Scicluna, B.P., Wolswinkel, R., de Jonge, B., Bezzina, C.R., Veldkamp, M.W., 2012. Functional Nav1.8 channels in intracardiac neurons: the link between SCN10A and cardiac electrophysiology. Circ. Res. 111, 333–343. https://doi.org/10.1161/CIRCRESAHA.112.274035.

Wang, D., Tai, P.W.L., Gao, G., 2019. Adeno-associated virus vector as a platform for gene therapy delivery. Nat. Rev. Drug Discov. 18, 358–378. https://doi.org/10.1038/s41573-019-0012-9.

Wright, A.F., 2015. Long-term effects of retinal gene therapy in childhood blindness. N. Engl. J. Med. 372, 1954–1955. https://doi.org/10.1056/NEJMe1503419.

Wu, Z., Asokan, A., Samulski, R.J., 2006. Adeno-associated virus serotypes: vector toolkit for human gene therapy. Mol. Ther. 14, 316–327. https://doi.org/10.1016/j.ymthe.2006.05.009.

Zeisel, A., Hochgerner, H., Lönnerberg, P., Johnsson, A., Memic, F., van der Zwan, J., Häring, M., Braun, E., Borm, L.E., La Manno, G., et al., 2018. Molecular Architecture of the Mouse Nervous System. Cell 174, 999–1014.e22. https://doi.org/10.1016/j.cell.2018.06.021.

Zhang, S., Gumpper, R.H., Huang, X.-P., Liu, Y., Krumm, B.E., Cao, C., Fay, J.F., Roth, B. L., 2022. Molecular basis for selective activation of DREADD-based chemogenetics. Nature 612, 354–362. https://doi.org/10.1038/s41586-022-05489-0.